Compact Tri-Band Antenna with Integrated Slot-Strip Filtering for Wi-Fi 7 Multi-Link Operation

Melissa Zebboudj[1,2], Jugurtha Derbah[1], Francis Keshmiri[1]
[1] Huawei Technologies, Boulogne-Billancourt, France, zebboudj.melissa@huawei.com
[2] EURECOM, Sophia Antipolis, France

***Abstract*— This paper presents a low-cost, compact tri-band antenna with an integrated filtering function, realized using a dual-PCB architecture for Wi-Fi 7 Access Point (AP) applications. The first PCB implements a dual-band array of two dipoles covering the 2.4 GHz and U-NII-1/2A [5.17–5.33 GHz] bands, the second PCB integrates a single-band array of three dipoles operating in the U-NII-3 [5.735–5.835 GHz] band. Filtering features are embedded in the antenna structure to suppress unwanted signals: the dual-band array rejects the U-NII-3 band, whereas the single-band array suppresses the U-NII-1/2A band through slots and strips. Decoupling rings provide strong port isolation, with measured S21 reaching –33 dB. The measured gains are 2.37 dBi, 3.23 dBi, and 3.21 dBi at 2.4 GHz, 5.2 GHz, and 5.78 GHz, respectively, while the radiation efficiency reaches about 63 %. Its compact size makes it suitable for Multi-Link Operation (MLO), enabling reliable Wi-Fi performance in multi-AP/multi-user FTTR deployments.**

***Index Terms—Tri-band* antennas, MLO, propagation, Filter antenna, FTTR, Wi-Fi 7.**

I. Introduction

The FTTR (*Fiber-To-The-Room*) solution enables the extension of fiber optic access into every room of a house through FTTR units. Each system typically includes a MFU (Master FTTR Unit) and several SFUs (Sub FTTR Units), ensuring optimal and stable Wi-Fi coverage, with each SFU connected to the splitter, which in turn is connected to the MFU, forming a centralized Point-to-Multi-Point (P2MP) topology [1-2]. This configuration enables unified management and reliable service delivery across all SFUs.

The antennas have a key role in the FTTR technology to provide flexible coverage and reliable Wi-Fi network to users who connect to MFU/SFUs. This requires antennas with fixed beams that can be directive or omni-directional [3], or reconfigurable antennas [4] which enable smart allocation of beams between multi-APs and the users, in residential [5] or Offices [6]. With the introduction of Wi-Fi 7, FTTR systems are evolving to support Multi-Link Operation (MLO), which enables simultaneous transmission and reception across multiple frequency bands (2.4 GHz, 5GHz U-NII-1/2A/3, as defined in IEEE 802.11 standard [7]). Achieving efficient MLO in compact FTTR units is challenging without antennas capable of transmitting co-band signals while suppressing cross-band interferences. Integrating filtering functions directly into the antenna represents a promising solution. Several approaches have been proposed in the literature. For instance, in [8], a patch antenna with U-slots and U-strips was used to implement a bandpass filter. In [9], slots on the patch and ground plane enabled a tri-band design by rejecting specific frequency bands. More recently, [10] proposed a passive patch antenna incorporating C-shaped slots to achieve three-pole rejection, providing strong suppression at critical coexisting Wi-Fi bands (4.9 GHz, 5.4 GHz, and 5.9 GHz) and maintaining over 5 dBi realized gain across the 5 GHz band.

Filtering antenna can be leveraged as a unique solution to enable simultaneous multi-band transmission and reception in compact FTTR systems. In this context, we propose a compact tri-band antenna with integrated filtering (*Filtenna*) for FTTR systems supporting Wi-Fi 7 operation in the 2.4 GHz and 5 GHz (low and high) bands. The antenna consists of U-shaped dipole arrays with slots and strips, designed to improve the channel quality between the MFU and SFUs. The design targets efficient co-band operation, strong out-of-band rejection, and low-cost fabrication for compact FTTR deployments.

II. Antenna design

A. Design objectives

Fig. 1 illustrates a typical MLO scenario in which two antennas of the same AP (ANT1 operating at f_1 and ANT2 operating at f_2). A station (STA1) receives the desired signal at frequency f_1 from ANT1, but also signal interference from ANT2 at the same frequency. Such overlap can degrade throughput and reliability. To mitigate this effect, ANT2 must reject the interfering frequency f_1.

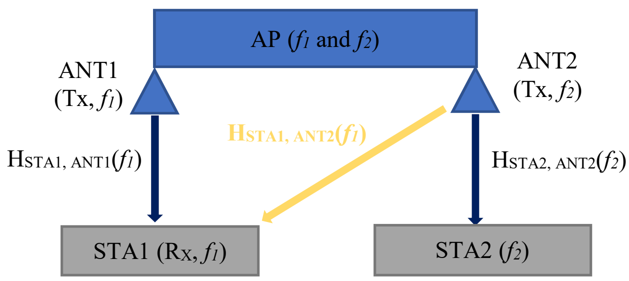

Fig. 1 Simultaneous transmission system model between AP and STAs, over two frequencies f_1 and f_2.

B. Antenna architecture

Fig. 2 shows the proposed antenna system with cover, which comprises two FR4 printed circuit boards (PCBs) with a relative permittivity of $\varepsilon_r = 4.4$ and a thickness of 0.4 mm, chosen to enable a low-cost fabrication.

Each PCB hosts multiple U-shaped dipole elements designed for specific frequency bands: PCB 1 covers two bands of 2.4 GHz and U-NII-1/2A (5.17–5.33 GHz), with integrated slots and strips to filter the U-NII-3 band. PCB 2 operates in single band U-NII-3 (5.735–5.835 GHz), employing strips and slots to reject the U-NII-1/2A band.

Each dipole array is fed through a coaxial cable. To minimize mutual coupling between the two PCBs, a decoupling ring structure is placed between them. The performance of the decoupling ring was evaluated by simulating a single ring element, applying appropriate port excitations and boundary conditions to analyze its reflection and transmission characteristics. This allowed us to predict the overall effect of the decoupling ring on reducing mutual coupling.

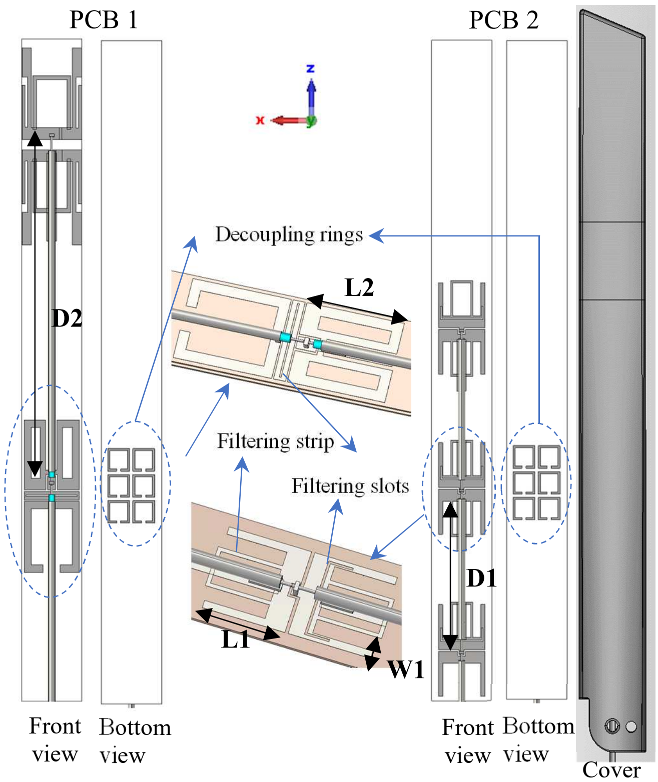

Fig. 2 Architecture of proposed antenna with two FR4 PCBs (ε_r=4.3, surface of 15cm by 1.4cm), placed within the cover with plastic ABS material (ε_r=3). Geometric parameters: L1=10.4mm, L2=16.2mm, W1=1mm, D1= 37.4mm, D2=83.59mm

C. Mechanisme of slot and strips

This section describes the operating principle of the slots and strips integrated into the antenna. Their dimensions are chosen to be approximately half the guided wavelength ($\lambda_g/2$) corresponding to the rejecting frequency.

To evaluate the effectiveness of this approach, simulations were performed on a single U-NII-3 antenna element both with and without the filtering structures. Fig. 3 presents the corresponding reflection coefficient (S_{11}) comparison.

The results indicate that the antenna with slots and strips remains well-matched in the U-NII-3 band, with $S_{11} < -10$ dB, while effectively rejecting the U-NII-1/2A band, where S_{11} approaches 0 dB. This confirms that the filtering elements enable efficient transmission in the desired band while minimizing inter-band interference.

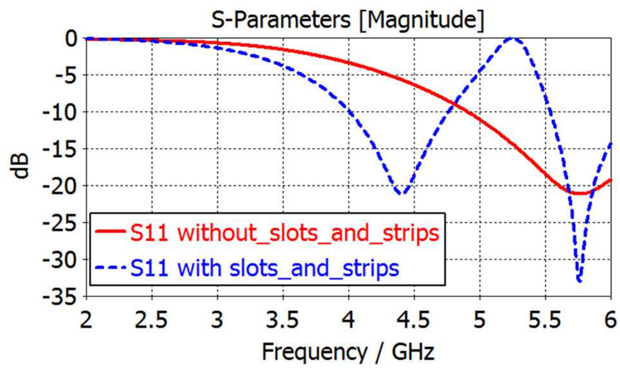

Fig. 3 Simulated return loss (S_{11}) with/without Slots and Strips.

III. Simulated Performance of Tri-Band Antenna

In this section, we present the simulation and measurement results for the proposed tri-band antenna, focusing on the role of the added elements (slots, strips, and decoupling elements) on antenna performance such as the gain, return loss, efficiency, and isolation. The simulations were carried out using CST Microwave Studio, with Port 1 assigned to the single-band U-NII-3 antenna and Port 2 to the dual-band antenna covering the 2.4 GHz and U-NII-1/2A bands.

A. Antenna Performance Review

Fig. 4 presents the simulated and measured performance of the proposed tri-band antenna, including reflection coefficients (S11 and S22), mutual coupling (S21), and total efficiency. Port 1 excites the U-NII-3 [5.735–5.835 GHz] band, while Port 2 feeds the dual-band antenna operating in the 2.4GHz and U-NII-1/2A [5.17–5.33 GHz] bands.

As shown in Fig. 4a and Fig. 4b, the reflection coefficients demonstrate good impedance matching in the desired frequency bands. Specifically, S11 remains below –10 dB for both simulation and measurement in the U-NII-3 band, while S22 stays below –10 dB in both 2.4GHz and U-NII-1/2A bands. Out-of-band rejection is also evident: in simulation, S11 exceeds –5 dB in the U-NII-1/2A band and –6 dB in the measurements, whereas S22 exceeds –5 dB in simulation and –6 dB in measurements in the U-NII-3 band. These results confirm the effectiveness of the integrated slots and strips in suppressing unwanted frequencies.

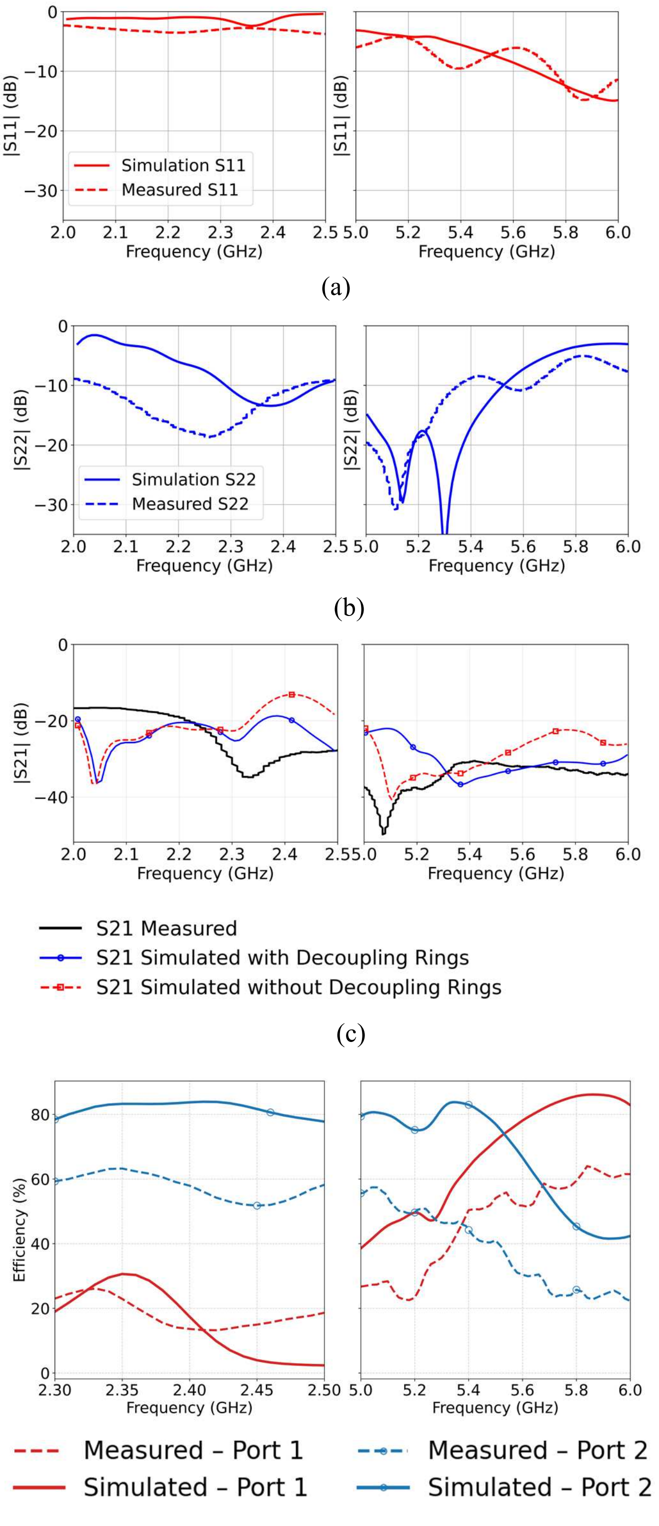

Fig. 4 Simulated and measured return loss of port 1 (a) and port 2 (b), isolation (c), and total efficiency (d) of the proposed Tri-band Antenna.

Fig. 4c shows the mutual coupling between the two antenna ports. Simulation results indicate that the introduction of decoupling rings improves isolation in the U-NII-3 band. With the decoupling rings, S21 remains below –27 dB across all operating bands, indicating strong isolation and minimal inter-antenna interference. In the measurements, the isolation is below –30 dB within the operating bands.

Fig. 4d presents both the simulated and measured radiation efficiencies across the frequency range. The simulated results show an efficiency higher than 80 % in the desired bands and below 50 % in the rejected bands, confirming the antenna's inherent filtering behavior.
The measured efficiency follows the same trend but reaches about 63 % in the operating bands. The difference between simulation and measurement can be attributed to fabrication tolerances, and connector or soldering losses. Furthermore, measurement uncertainties and setup imperfections may also contribute to this deviation. Nevertheless, the overall behavior remains consistent, with high efficiency in the passbands and very low radiation efficiency in the rejected bands, validating the filtering characteristics of the proposed antenna.

B. Realized Gain in Desired and Rejected Bands

Fig. 5 presents the simulated and measured normalized radiation patterns of the proposed tri-band antenna in the desired and undesired frequency bands. The simulated gains are 3.33 dBi at 2.4 GHz, 3.78 dBi at 5.2 GHz (center of U-NII-1/2A), and 4.05 dBi at 5.78 GHz (center of U-NII-3) in the desired bands. The corresponding measured gains are 2.37 dBi, 3.23 dBi, and 3.21 dBi, respectively. The slight differences between simulation and measurement are mainly due to coaxial cable losses, fabrication tolerances, and measurement setup uncertainties. However, the measured patterns exhibit similar shapes and main lobes as the simulations, confirming efficient radiation in all operating bands.

For undesired bands, both simulation and measurement indicate good rejection, with measured gains of 0.77 dBi at 2.4 GHz, −0.85 dBi at 5.2 GHz, and 0.65 dBi at 5.78 GHz. The low radiation observed in these bands can be attributed to the influence of the coaxial cable, which can slightly disturb the current distribution of the antenna. Overall, the results confirm that the proposed antenna radiates effectively in the intended frequency ranges while effectively suppressing out-of-band emissions.

The presented results confirm the antenna's embedded filtering behavior, and demonstrate excellent band isolation and suitability for reliable Multi-Link Operation (MLO) in Wi-Fi 7 applications. The prototype of the fabricated tri-band antenna is shown in Fig. 6.

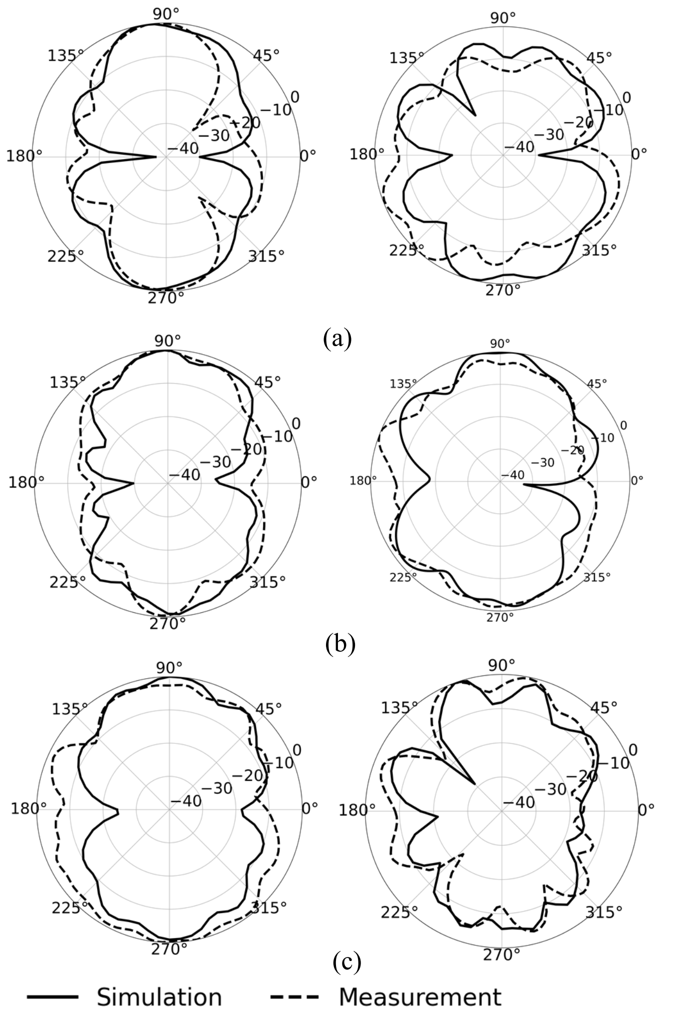

Fig. 5 Simulated and measured E-plane (φ = 0°) radiation patterns of the tri-band antenna at (a) 2.4, (b) 5.2, and (c) 5.8 GHz (PCBs along z-axis). Left the wanted bands and right the unwanted bands

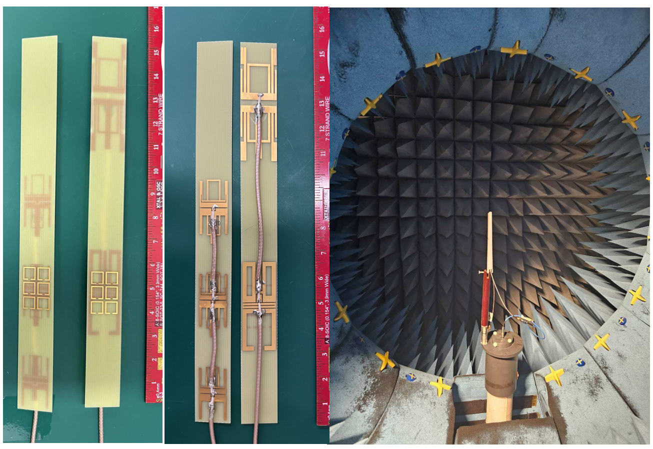

Fig. 6 Prototype of the fabricated tri-band antenna

IV. Conclusion

A compact tri-band antenna with an integrated filtering function is presented. The design employs a dual-PCB architecture operating in the 2.4 GHz, 5.17–5.33 GHz, and 5.735–5.835 GHz Wi-Fi bands. The antenna enables co-band signal transmission while suppressing cross-band interference through embedded slots and strips. Decoupling rings implemented on the PCBs provide strong isolation, with the measured S21 reaching –33 dB, compared to –27 dB in simulation. The measured realized gains are 2.37 dBi, 3.23 dBi, and 3.21 dBi at 2.4, 5.2, and 5.78 GHz, respectively, in good agreement with simulations. The measured radiation efficiency reaches about 63 %, slightly lower than simulated values partly due to variations of the conductor and dielectric losses as well as the effects from the measurement setup with radiating cables which could not be modeled precisely. Both simulation and measurement confirm stable radiation patterns and effective suppression of out-of-band radiation. Having compact size and robust filtering behavior, the proposed antenna is a promising antenna candidate for Wi-Fi 7 access points units.

References

[1] GSTP-FTTR Use cases and requirements of FTTR, ITU-T, Apr. 2021

[2] ETSI GR F5G 002, F5G Use Cases standard, Release #3, Jun. 2024

[3] Y. Dong, J. You and F. Keshmiri, "Review on the New Antenna Evolution for Next Generation WiFi-7/8 Systems," 2025 19th European Conference on Antennas and Propagation (EuCAP), Stockholm, Sweden, 2025.

[4] C. D. Giovampaola, F. Keshmiri, F. Caminita, Y. Zeng and S. Maci, "Low-Profile Wi-Fi Antenna with Reconfigurable Metasurface for FTTR Applications," 2025 19th European Conference on Antennas and Propagation (EuCAP), Stockholm, Sweden, 2025

[5] F. Keshmiri, H. Xiong, Z. Ren, "Smart antenna for optical network terminals and indoor optical network" WO2024007210A1

[6] C. Chen, X. Xu, L. Zhang and F. Keshmiri, "Compact Horizontally Polarized Dual-Beam Antenna with Large Tilted Beam Angle for FTTR Applications," 2025 19th European Conference on Antennas and Propagation (EuCAP), Stockholm, Sweden, 2025

[7] IEEE Standard for Information Technology—Telecommunications and information exchange between systems Local and metropolitan area networks—Specific requirements—Part 11: Wireless LAN Medium Access Control (MAC) and Physical Layer (PHY) Specification, 2021

[8] Yang et al., "A Simple, Compact Filtering Patch Antenna Based on Mode Analysis With Wide Out-of-Band Suppression," in IEEE Transactions on Antennas and Propagation, vol. 67, no. 10, pp. 6244-6253, Oct. 2019, doi: 10.1109/TAP.2019.2922770.

[9] D. D. Krishna, M. Gopikrishna and C. K. Aanandan, "A CPW-fed Triple Band Monopole Antenna for WiMAX/WLAN Applications," 2008 38th European Microwave Conference, Amsterdam, Netherlands, 2008, pp. 897-900, doi: 10.1109/EUMC.2008.4751598.

[10] Y. Dahmani and F. Keshmiri, "C-Slotted Patch Filter Antenna with Triple Notches for Enhanced Wi-Fi Performance," 2025 19th European Conference on Antennas and Propagation (EuCAP), Stockholm, Sweden, 2025, pp. 1-4, doi: 10.23919/EuCAP63536.2025.11000011.